AXIAL SPEED OF SOUND IS RELATED TO TENDON'S NONLINEAR ELASTICITY

Claudio Vergari[a,*], Bérangère Ravary-Plumioën[a], Delphine Evrard[a], Pascal Laugier[b], David Mitton[c]

Philippe Pourcelot[a] and Nathalie Crevier-Denoix[a]

Abstract

Axial speed of sound (SOS) measurements have been successfully applied to noninvasively evaluate tendon load, while preliminary studies showed that this technique also has a potential clinical interest in the follow up of tendon injuries. The ultrasound propagation theory predicts that the SOS is determined by the effective stiffness, mass density and Poisson's ratio of the propagating medium. Tendon stiffness characterizes the tissue's mechanical quality, but it is often measured in quasi-static condition and for entire tendon segments, so it might not be the same as the effective stiffness which determines the SOS.

The objectives of the present study were to investigate the relationship between axial SOS and tendon's nonlinear elasticity, measured in standard laboratory conditions, and to evaluate if tendon's mass density and cross-sectional area (CSA) affect the SOS level.

Axial SOS was measured during in vitro cycling of 9 equine superficial digital tendons. Each tendon's stiffness was characterized with a tangent modulus (the continuous derivative of the true stress / true strain curve) and an elastic modulus (the slope of this curve's linear region).

Tendon's SOS was found to linearly vary with the square root of the tangent modulus during loading; tendon's SOS level was found correlated to the elastic modulus's square root and inversely correlated to the tendon's CSA, but it was not affected by tendon's mass density. These results confirm that tendon's tangent and elastic moduli, measured in laboratory conditions, are related to axial SOS and they represent one of its primary determinants.

Keywords: Tendon; Quantitative ultrasound; Speed of sound; Elastic modulus; Mechanical properties.

[a] Université Paris-Est, Ecole Nationale Vétérinaire d'Alfort, USC BPLC 957, Maisons-Alfort, F-94704, France; INRA, USC BPLC 957, Maisons-Alfort, F-94704, France.

[b] UPMC Univ Paris 6, UMR CNRS7623, LIP, Paris, F-75005 France.

[c] Université de Lyon, F-69622, Lyon, France; IFSTTAR, LBMC, UMR_T9406, F-69675, Bron; Université Lyon 1, Villeurbanne

*Corresponding author: c.vergari@gmail.com (C.Vergari)

1

1. Introduction

Axial speed of sound (SOS) in tendon is still an underexploited field of quantitative ultrasound although it shows great potential for biomechanical research and clinical application. For instance, SOS measurements are currently being applied to non-invasively evaluate tendon load (Pourcelot et al., 2005a) during locomotion; the influence of track surface on equine superficial digital flexor tendons (SDFT) has been investigated with this technique (Crevier-Denoix et al., 2009a), while preliminary results have been reported for load evaluation in human Achilles tendons (Pourcelot et al., 2005b; Roux and Defontaine, 2005). Moreover, preliminary studies have been performed to evaluate the potential of axial SOS measurement in the follow-up of tendon lesions (Vergari et al., 2012a; Vergari et al., 2012b).

This technique, based on the speed measurement of ultrasound signals propagating in the tendon's axial direction, was originally developed for bone properties assessment (Foldes et al., 1995; Lowet and Van der Perre, 1996). It has been demonstrated that SOS in tendon varies nonlinearly with the applied load (Pourcelot et al., 2005a); this nonlinear relation was very similar in shape among different tendons (Crevier-Denoix et al., 2009b), but each tendon's SOS chart was separated from the others, almost systematically along the chart (enabling the definition of the "SOS level" of the chart).

Bossy et al. (2002) demonstrated that the apparent SOS in axial transmission, applied to thick bone cortex (i.e. much thicker than the involved wavelength), corresponds to the speed of compressional bulk waves. For a lossless isotropic medium (Rose, 2004):

$$SOS = \sqrt{\frac{E}{\rho} \frac{1-\upsilon}{(1+\upsilon)(1-2\upsilon)}} \qquad (1)$$

where ρ is the medium's mass density, ν is its Poisson's ratio (the negative ratio of axial on transversal strain) and E is its effective stiffness; the latter represents the medium's elastic response to the dynamic excitation of the ultrasound waves at the wavelength scale (about 2 mm in current axial SOS applications, which utilize 1 MHz signals). It was previously observed that the average equine SDFT Poisson's ratio is 0.55 (Vergari et al., 2011), and that it does not significantly vary with load. While isotropic materials cannot have Poisson's ratios higher than 0.5, this is quite common in transversely isotropic materials (Jones, 1999; Lempriere, 1968). A Poisson's ratio near 0.5 implies that volume variations, and thus mass density variations, are negligible during loading (in absence of mass losses); given that these hypotheses are true, SOS should be proportional to the square root of tendon's effective stiffness during loading (Eq. 1).

Stiffness is an important parameter to describe tendon's mechanical quality and, in presence of an injury, its health status (Crevier-Denoix et al., 1997); this parameter is usually measured by mechanical testing under quasi-static conditions and for entire tendon segments (i.e. at much larger scale than the wavelength, Abrahams, 1967; Crevier et al., 1996; Gillis et al., 1995; Riemersma and Schamhardt, 1985). These conditions significantly differ from the dynamic excitation imposed by ultrasound waves at wavelength scale. Tendon stiffness varies with the applied load, so it can be characterized in a variety of ways; for instance it can be modelled as a tangent modulus (i.e. the instantaneous derivative of the tendon's stress/strain curve), which is a continuous function varying with axial load (or strain). Or, tendon stiffness can be described as an elastic modulus, a single value that averages the slope of the linear region in the stress/strain curve. Therefore, it is not clear if tendon stiffness, thus measured and defined, is similar to the effective stiffness that determines the speed of ultrasound waves in axial propagation. Still, the major interest for tendon's biomechanics research and clinical application lies in the tangent or elastic modulus, and not in the effective stiffness appearing in Eq. 1.

The objectives of the present work were to assess if tendon stiffness, measured in standard laboratory conditions, is related to the SOS level in the SDFT and to determine if this nonlinear
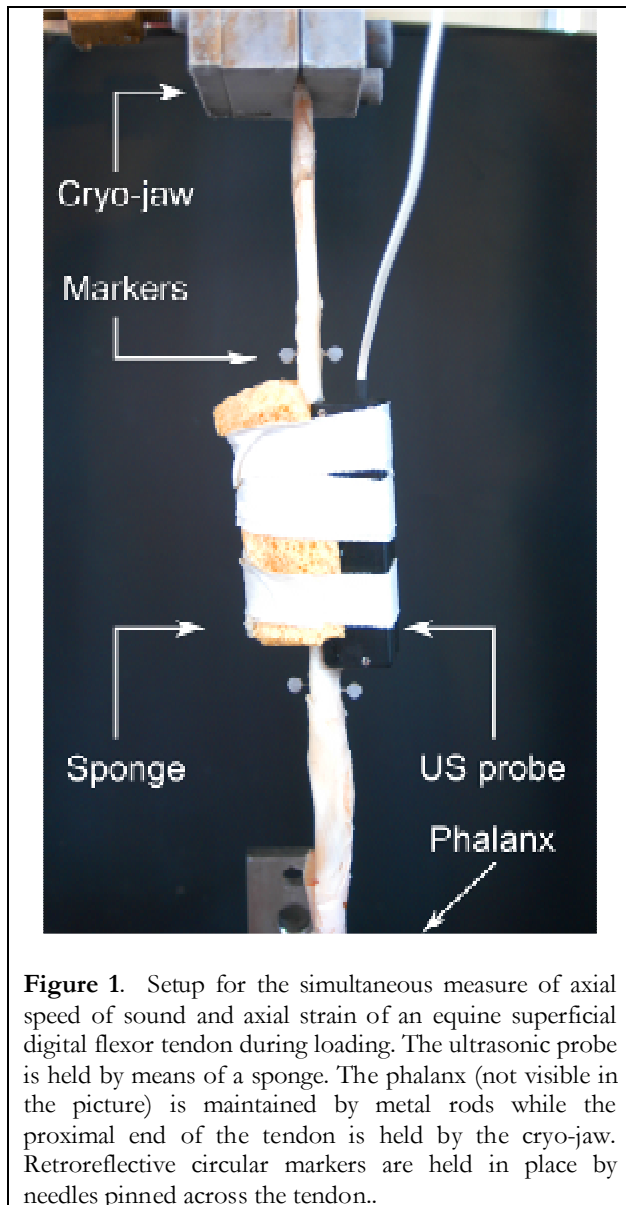
Figure 1. Setup for the simultaneous measure of axial speed of sound and axial strain of an equine superficial digital flexor tendon during loading. The ultrasonic probe is held by means of a sponge. The phalanx (not visible in the picture) is maintained by metal rods while the proximal end of the tendon is held by the cryo-jaw. Retroreflective circular markers are held in place by needles pinned across the tendon..

elastic parameter is a primary determinant of SOS variations with load; as a secondary objective, SOS level was also compared to tendon's mass density and cross-sectional area (CSA).

2. Materials and methods

2.1 Tendons

Nine superficial digital flexor tendons (SDFT) were isolated from the forelimbs' carpal area of 5 horses (517.6 ± 74.1 kg average body weight; 8.4 ± 3.6 years of age, Table 1) which had been put down for reasons independent from this study. The tendons were free of tendinitis (based on inspection, palpation and ultrasonographic examination); 4 of them were tested within 4 h post-mortem, whereas the others were preserved by freezing in plastic bags (before dissection) for several days to 13 weeks prior to the tests (Table 1). The tendons were thawed the day before the test and isolated (just before the test) preserving the distal insertion on the middle phalanx.

2.2 Experimental apparatus and protocol

The tendons' cross-sectional areas at rest (CSA_0) were measured ex vivo by ultrasonography, with the tendon slightly taut and immersed in water. Each tendon was then installed on a testing machine (10/MH, MTS Systems Corporation, Eden Prairie, MN USA) by clamping its proximal end in a cryo-jaw (Riemersma and Schamhardt, 1982) and by blocking the phalanx with metal rods.

A previously described 1 MHz US probe (Pourcelot et al., 2005a) was installed on the palmar aspect of the tendon and secured with adhesive bands to a sponge placed on the opposite side of the tendon (Fig. 1). SOS was calculated from the times of flight of the first arriving signal measured between 2 receivers (separated by 13.65 mm); the signal's arrival was detected using an intercorrelation method.

The length of the tendon's segment of interest during the mechanical test was measured with a previously described technique (Crevier et al., 1996). Briefly, two needles were transversely inserted across the tendon, separated by about 12 cm in the axial direction (Fig. 1). The extremities of the needles were equipped with circular retroreflective markers which were filmed during the test with a video camera placed at about 3 m from the plane formed by the four markers, at the same height as the US probe. The instantaneous length (L) of the segment of interest was assessed by measuring on each film frame the distance between the middle points of each couple of markers. The segment's length at rest (L_0) was evaluated from the length/force curve at a 50 N load. The force signal was provided by the testing machine's 50kN load cell.

Each tendon was preconditioned with 10 loading/unloading cycles between 50 and 2500 N. Continuous loading/unloading cycles were then started at a constant speed of 500 mm/min (about 2% axial strain/s); axial SOS and elongation were measured during 15 seconds (corresponding to about 3 cycles). Tendons #1 and #2 were cycled between 50 and 8000 N (since they presented larger CSAs) while the others between 50 and 5500 N.

2.3 Data acquisition and analysis

SOS and tendon's axial load were synchronously acquired at 100 Hz, while the video recordings (i.e., the tendon's length) was performed at 25 Hz; all data were thus resampled at 25 Hz and synchronized by aligning the first peak of the tendon load and length during cycling.

True stress was defined as $\sigma = F/[CSA_0(1+\varepsilon)^{-2*0.55}]$, where F is the tendon's axial load and ε is the axial true strain ($\varepsilon = \ln(L/L_0)$). This definition assumes that tendon's Poisson's ratio is 0.55 (Vergari et al., 2011). Each true stress/strain curve was approximated with a 3rd order polynomial, the derivative of which represents the tendon's
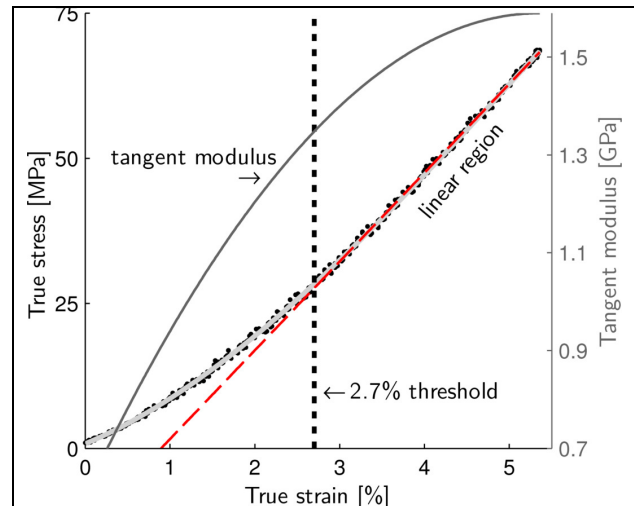

Figure 2. Experimental points (corresponding to 3 loading/unloading cycles) and 3rd degree polynomial approximation of the true stress/strain curve of tendon #1 (left ordinates axis) and corresponding tangent modulus (right ordinate axis). The red dashed line represents the slope of the almost linear region.

tangent modulus.

The relation between the SOS and the square root of the tangent modulus (SRTM) of each tendon was linearly approximated; the root mean square error (RMSE) between this linear model and the experimental points was calculated for each tendon in order to quantify the relation's linearity.

The tendon's elastic modulus (E_L) was defined as the linear slope of the true stress / true strain curve for strains higher than 2.7 % (Fig. 2), and it was calculated for each tendon in order to characterize their stiffness (Riemersma and Schamhardt, 1985). The lower strain threshold was fixed at 2.7 % since it was previously observed that tendon's Poisson's ratio at higher strain does not significantly vary with load (Vergari et al., 2011). The elastic modulus approximated for small deformations (E_S), which can be compared with previous literature data, was calculated as the linear slope of the engineering stress (F/CSA_0) versus engineering strain (($L-L_0$)/L_0) curve, for strains higher than 2.7 %.

Table 1. Origin and characteristics of the 9 equine superficial digital flexor tendons tested.

#	Horse				Tendon		
	Breed	Age [years]	Weight [kg]	Limb	CSA [mm²]	Density [Kg/m³]	Freezing duration [weeks]
1	Cob	6	619	R	120	1110	2
2	Cob	6	619	L	123	1100	2
3	TB	16	518	R	99	1060	14
4	SB	8	414	R	65	1060	fresh
5	SB	8	414	L	68	1150	fresh
6	SF	11	540	R	95	1070	11
7	SF	11	540	L	107	1120	13
8	SB	5	497	R	77	1110	fresh
9	SB	5	497	L	74	1130	fresh
Mean		8	517		92	1101	
SD		4	74		22	31	

CSA: Cross-sectional area; TB: Thoroughbred; SF: Selle français; SB: Standardbred; R: Right forelimb; L: Left forelimb.

The SOS level of each tendon was evaluated as an asymptotic value (SOS_A). SOS_A was calculated by approximating the SOS / true strain curve with an exponential function in the form $SOS = SOS_A\left(1 - \alpha e^{-\beta\varepsilon}\right)$, where the parameters α and β where optimized for each tendon.

Mass density was assessed for each tendon's after the mechanical test by hydrostatic weighting of a 7 cm sample cut from the centre of the segment of interest.

Normality was tested with the Lilliefors test, Pearson's correlation coefficient and linear regression were utilized to evaluate the relationship between variables; Spearman's rank correlation coefficient was adopted to evaluate variables' relation with the freezing time, since it was not normally distributed. Statistical

significance was accepted at $p < 0.05$.

3. Results

Experimental results are reported in Tables 1 and 2. The average SOSA difference between right and left SDFT of the same horse was 14 ± 9 m/s (ranging from 1 m/s between tendons #1 and #2 to 23 m/s between tendons #6 and #7).

Fig. 3 shows the SOS as a function of axial load, true stress and true strain. While SOS variation with load (or true stress and strain) was nonlinear, its relation with the square root of the tangent modulus (SRTM) was almost linear (Fig.4), with an average RMSE between the actual data and the linear approximation of 9.9 m/s. This RMSE was found inversely correlated
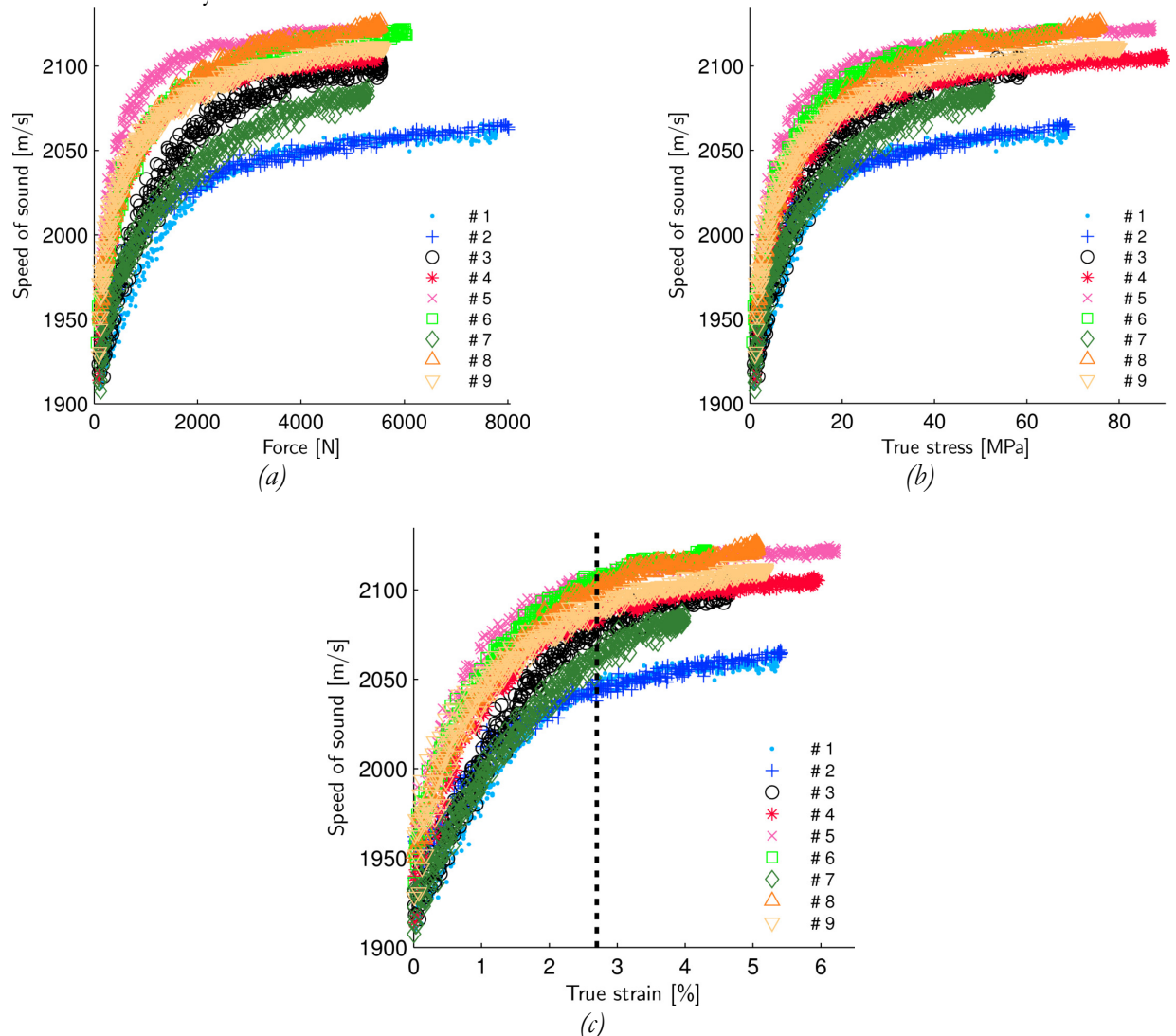

Figure 3. Axial speed of sound in 9 superficial digital flexor tendons plotted against (a) axial load, (b) true stress and (c) true strain. Each curve represents three loading/unloading cycles, while the vertical dotted line in (c) represents the 2.7 % true strain threshold. Tendons coming from the same horse share similar colour codes.
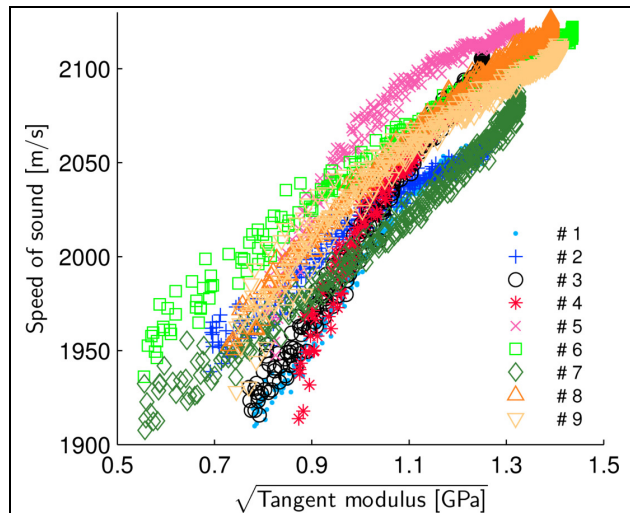
Vergari et al.   5

Figure 4. Axial speed of sound in 9 superficial digital flexor tendons plotted against the square root of the tendons' tangent modulus. Each curve represents three loading/unloading cycles. Tendons coming from the same horse share similar colour codes.

to the freezing time (Spearman's rho = -0.72, p = 0.039), the freezing time of the fresh tendons being considered equal to 0.

A significant correlation was found between SOS_A and the square root of E_L (r = 0.75, p = 0.019, Fig. 5); the correlation between SOS_A and the square root of E_S was similar (r = 0.74, p = 0.022). SOS_A was also found inversely correlated to the tendons' CSA at rest (Fig.6), while no correlation was found with tendon's mass density (Fig.7).

4. Discussion

Axial SOS was measured in 9 SDFTs during loading in order to investigate the relation between the SOS and tendon stiffness, which was measured in quasi-static conditions. It was observed that SOS is linearly related to the square root of the tendon's tangent modulus. Moreover, the tendons' SOS level was correlated to the square root of the tendons' elastic modulus. The measured SOS / load curves were similar to those previously observed for SDFTs in isolated limbs and isolated tendons (Crevier-Denoix et al., 2009b; Pourcelot et al., 2005a).

The reproducibility of axial SOS measurement in equine SDFTs was recently evaluated *in vitro*

(Crevier-Denoix et al., 2009b); all the tested tendons showed a similar nonlinear relation between SOS and tendon load, but relatively large differences in SOS level (100 m/s at 1100 N) were observed between different tendons. The largest differences observed at 1100 N in the present study was similar (103 m/s) while the largest difference in SOS_A was 62 m/s. The variability of SOS_A observed in the present *in vitro* study between tendons coming from the same subject (14 m/s in average) is similar to the one previously found (Crevier-Denoix et al., 2009b). This suggests that it might not be advisable to use the contralateral limb as a SOS reference when, for instance, the normal tendon SOS needs to be evaluated in presence of a unilateral lesion (Vergari et al., 2012a). However, the tendons' pairs from the same subject were not measured in the same conditions: the two pairs of fresh tendons were tested a few hours from each other (maximum 4 hours), while tendon #8 was preserved frozen 2 weeks more than #7. Moreover, the sensitivity if the measurements to the probe positioning has not been evaluated yet. Therefore, this difference in asymptotic SOS between pairs of tendons from the same subject should be further investigated with *in vivo* measurements.

Tangent modulus and elastic modulus are two different descriptions of tendon's mechanical behaviour: the former models the continuous derivative of the nonlinear relation between
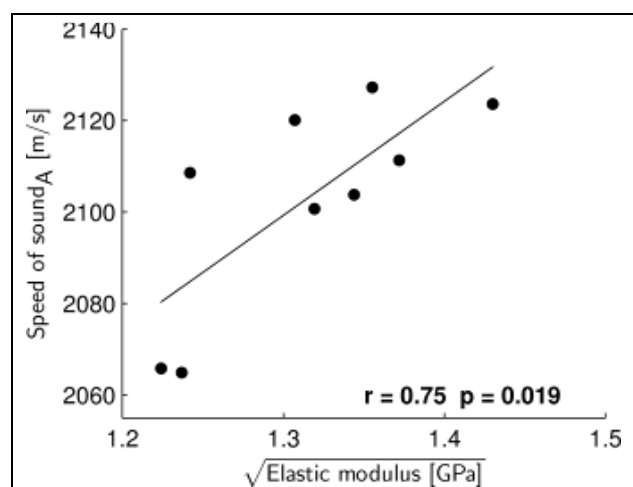

Figure 5. Asymptotic axial speed of sound in 9 superficial digital flexor tendons plotted against the square root of tendon's linear elastic modulus.
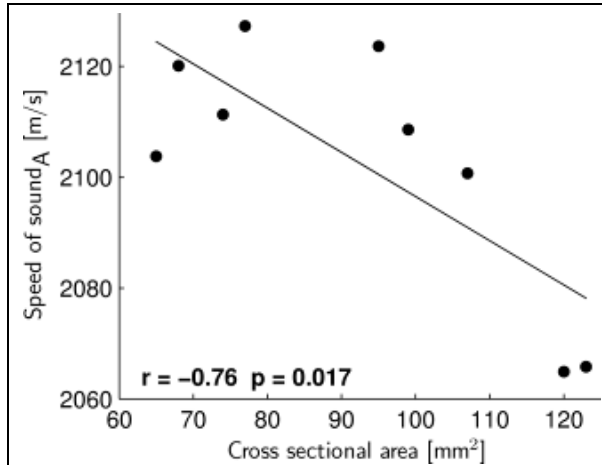
Figure 6. Asymptotic axial speed of sound in 9 superficial digital flexor tendons plotted against the tendon's cross-sectional area at rest.
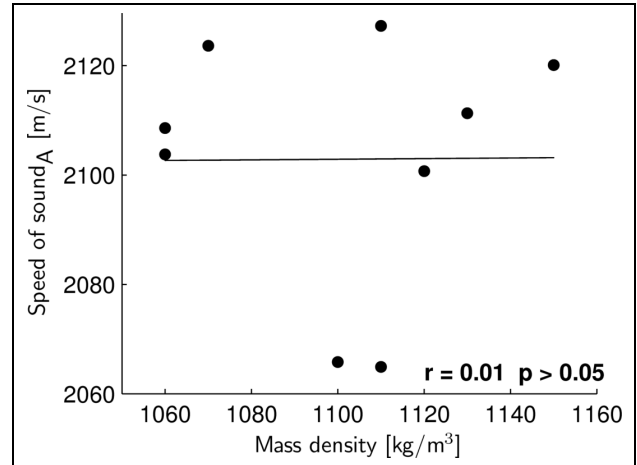

Figure 7. Asymptotic axial speed of sound in 9 superficial digital flexor tendons plotted against tendon mass density; no significant correlation was observed.

stress and strain, while the latter grossly characterizes tendon stiffness and enables a direct comparison between tendons or with other variables (such as SOS_A). Similarly, each tendon's SOS level was quantified by evaluating an asymptotic value, although the SOS is still almost linearly increasing at the maximal strains applied in this study.

It is well known that tendon's elastic stress/strain curves present a toe region (due to the straightening of the tendon fibres crimps) followed by a linear region, but the transition between the two is generally arbitrary and depend on the definition of the sample's initial length. Abrahams (1967) observed that the stress/strain relation of SDFTs became linear beyond 3 % engineering strain, while Riemersma and Schamhardt (1985) fixed a threshold at 2 % engineering strain. In the present article, a threshold was fixed at 2.7 % true strain (the difference with the engineering strain being 0.036 %) since it was previously observed that tendon Poisson's ratio at higher strain does not significantly vary with load (Vergari et al., 2011); this assures that the effects of Poisson's ratio on the SOS variation in the linear region are minimal. The average elastic modulus approximated for small deformations was 1.54 ± 0.17 GPa, which is consistent with previous studies (Crevier-Denoix et al., 2005; Gillis et al., 1995; Riemersma and Schamhardt, 1985).

Tendon stiffness was assessed in quasi-static testing and on entire tendons, although ultrasound waves are affected by the tendon's material properties at wavelength scale and at the proper frequency; moreover, the stiffness appearing in Eq. 1 represents the elastic response to the tiny mechanical perturbations induced by the propagating waves, while tendon stiffness was evaluated in large deformations. These conditions rend the measured tendon stiffness a rough approximation of the value appearing in Eq. 1. Besides, Eq. 1 is valid for isotropic materials, while tendon has a transversely isotropic behaviour; SOS should more appropriately be expressed as:

$$SOS_{TransIsotropy} = \sqrt{\frac{E}{\rho} \frac{(1 - \upsilon_{TT})}{(1 - \upsilon_{TT} - 2\upsilon_{TA}\upsilon)}} \quad (2)$$

where υ_{TT} is the negative ratio of transverse orthogonal strain on transverse strain in uniaxial transversal tension, and υ_{TA} is the negative ratio of axial strain on transverse strain in uniaxial transversal tension. These two parameters have not been studied yet in SDFT.

Because of the relatively large deformation involved, true stress and strain were initially preferred, over their approximated engineering values, to evaluate tendon stiffness, although eventually both showed the same relationships with axial SOS. Tendon CSA variation with axial strain was evaluated by assuming that tendon's Poisson's ratio was 0.55, since it was

Table 2. Asymptotic speed of sound (SOS$_A$), linear elastic modulus (E$_L$) and linear elastic modulus approximated for small deformations (E$_S$).

#	SOS$_A$ [m/s]	E$_L$ [GPa]	E$_S$ [GPa]
1	2065	1.53	1.36
2	2066	1.50	1.33
3	2109	1.54	1.38
4	2104	1.81	1.59
5	2120	1.71	1.50
6	2124	2.04	1.85
7	2101	1.74	1.58
8	2127	1.84	1.64
9	2111	1.88	1.68
Mean	2103	1.73	1.54
SD	23	0.18	0.17

previously shown that such approximation reduces the error introduced by the engineering stress for large deformations (Vergari et al., 2011).

SOS$_A$ was correlated to tendon's elastic modulus ($p = 0.019$), confirming that the quasi-static measurement of tendon's stiffness is related to the effective stiffness which determines the SOS (Eq. 1). SOS$_A$ was not correlated to mass density, nor with its reciprocal (as it appears in Eq.1); this is probably due to the fact that mass density was rather homogeneous among tendons (coefficient of variation = 2.9 %), unlike the elastic modulus (coefficient of variation = 12.0 %). A correlation was also observed between the SOS level and tendon's CSA; this merits to be further investigated since the initial hypotheses were that SOS would not depend on tendon structure, but only on its material properties.

The maximal RMSE of the linear approximation of the SOS/SRTM curves was 14 m/s (0.7 % of the average SOS$_A$), indicating that SOS varies linearly with the square root of the tangent modulus. The four fresh tendons tested in the present study, however, presented less linear curves (Fig. 4); more precisely, the RMSE was found inversely correlated with the freezing period ($p = 0.039$). Contradictory findings on the effects of freezing connective tissues have been reported in the literature (Clavert et al., 2001; Giannini et al., 2008; Viidik and Lewin, 1966; Woo et al., 1986); it is possible that freezing could affect the tendon's mechanical properties, especially since it can provoke tissue dehydratation and it was reported that SDFT water content is correlated to tendon SOS (Miles et al., 1996). In particular, fluid exudation in presence of higher water content might provoke a non-negligible mass loss during loading; the induced tissue density variations could affect the SOS, although the repeatability of the SOS/SRTM curves during load cycling undermines this hypothesis. The fresh tendons were tested within 4 hours from the animal's death, so dehydratation was minimized; however, it can be expected that if the SOS/SRTM relation could be directly assessed *in vivo*, it would be more nonlinear.

Poisson's ratio participation in the SOS variation with load is likely negligible, since it was found that this ratio does not significantly vary with load and that the square root of the tendon tangent modulus varies linearly with SOS. The precision error of the cited Poisson's ratio measurement (15.1 % with 95 % confidence interval. Vergari et al., 2011), however, is not small enough to exclude that this parameter might slightly vary with load, thus influencing SOS variations in the linear region.

5. Conclusions

The relations of axial SOS with the nonlinear elastic properties, tendon mass density and CSA of the equine SDFT were investigated in the present study. The results show that tendon stiffness, assessed in standard laboratory conditions, was related to both the axial SOS variation with load and the SOS level. These results open new possibilities of axial SOS applications in tendon for biomechanics research and they confirm its clinical interest in the evaluation of injured tendon's healing, which should be now investigated further.

Conflict of interest statement

The authors have no conflicts of interest to disclose.

Acknowledgments

References

Abrahams, M., 1967. Mechanical behaviour of tendon in vitro. A preliminary report. Medical and Biological Engineering and Computing 5, 433-443.

Clavert, P., Kempf, J. F., Bonnomet, F., Boutemy, P., Marcelin, L., Kahn, J. L., 2001. Effects of freezing/thawing on the biomechanical properties of human tendons. Surgical and Radiologic Anatomy 23, 259-262.

Crevier-Denoix, N., Collobert, C., Pourcelot, P., Denoix, J. M., Sanaa, M., Geiger, D., Bernard, N., Ribot, X., Bortolussi, C., Bousseau, B., 1997. Mechanical properties of pathological equine superficial digital flexor tendons. Equine Veterinary Journal Supplements, 23-26.

Crevier-Denoix, N., Pourcelot, P., Ravary, B., Robin, D., Falala, S., Uzel, S., Grison, A. C., Valette, J. P., Denoix, J. M., Chateau, H., 2009a. Influence of track surface on the equine superficial digital flexor tendon loading in two horses at high speed trot. Equine Veterinary Journal 41, 257-261.

Crevier-Denoix, N., Ravary-Plumioën, B., Evrard, D., Pourcelot, P., 2009b. Reproducibility of a non-invasive ultrasonic technique of tendon force measurement, determined in vitro in equine superficial digital flexor tendons. Journal of Biomechanics 42, 2210-2213.

Crevier-Denoix, N., Ruel, Y., Dardillat, C., Jerbi, H., Sanaa, M., Collobert-Laugier, C., Ribot, X., Denoix, J. M., Pourcelot, P., 2005. Correlations between mean echogenicity and material properties of normal and diseased equine superficial digital flexor tendons: an in vitro segmental approach. Journal of Biomechanics 38, 2212-2220.

Crevier, N., Pourcelot, P., Denoix, J. M., Geiger, D., Bortolussi, C., Ribot, X., Sanaa, M., 1996. Segmental variations of in vitro mechanical properties in equine superficial digital flexor tendons. American Journal of Veterinary Research 57, 1111-1117.

Foldes, A. J., Rimon, A., Keinan, D. D., Popovtzer, M. M., 1995. Quantitative ultrasound of the tibia: a novel approach for assessment of bone status. Bone 17, 363-367.

Giannini, S., Buda, R., Di Caprio, F., Agati, P., Bigi, A., De Pasquale, V., Ruggeri, A., 2008. Effects of freezing on the biomechanical and structural properties of human posterior tibial tendons. International Orthopaedics 32, 145-151.

Gillis, C., Sharkey, N., Stover, S. M., Pool, R. R., Meagher, D. M., Willits, N., 1995. Effect of maturation and aging on material and ultrasonographic properties of equine superficial digital flexor tendon. American Journal of Veterinary Research 56, 1345-1350.

Jones, R. M. 1999. Mechanics of composite materials, Taylor & Francis Inc., Philadelphia, PA, USA.

Lempriere, B. M., 1968. Poisson's ratio in orthotropic materials. American Institute of Aeronautics and Astronautics Journal 6, 2226-2227.

Lowet, G., Van Der Perre, G., 1996. Ultrasound velocity measurement in long bones: measurement method and simulation of ultrasound wave propagation. Journal of Biomechanics 29, 1255-1262.

Miles, C. A., Fursey, G. A. J., Birch, H. L., Young, R. D., 1996. Factors affecting the ultrasonic properties of equine digital flexor tendons. Ultrasound in Medicine & Biology 22, 907-915.

Pourcelot, P., Defontaine, M., Ravary, B., Lematre, M., Crevier-Denoix, N., 2005a. A non-invasive method of tendon force measurement. Journal of Biomechanics 38, 2124-2129.

Pourcelot, P., Van Den Bogert, A. J., Huang, X., Crevier-Denoix, N. 2005b. Achilles and patellar tendon loading during gait measured using a non-invasive ultrasonic technique. In International Society of Biomechanics XXth Congress - ASB 29th Annual Meeting. Cleveland, Ohio, USA.

Riemersma, D. J., Schamhardt, H. C., 1982. The cryo-jaw, a clamp designed for in vitro rheology studies of horse digital flexor tendons. Journal of Biomechanics 15, 619-620.

Riemersma, D. J., Schamhardt, H. C., 1985. In vitro mechanical properties of equine tendons in relation to cross-sectional area and collagen content. Research in Veterinary Science 39, 263-270.

Rose, J. L. 2004. Ultrasonic Waves in Solid Media, Cambridge University Press.

Roux, C., Defontaine, M. 2005. Ultrasonic measurement of the human achilles tendon stress during loading: preliminary experimental and theoretical results. In Ultrasonics Symposium. Rotterdam.

Vergari, C., Pourcelot, P., Holden, L., Ravary-Plumioën, B., Gerard, G., Laugier, P., Mitton, D., Crevier-Denoix, N., 2011. True stress and Poisson's ratio of tendons during loading. Journal of Biomechanics 44, 719-724.

Vergari, C., Pourcelot, P., Ravary-Plumioën, B., Dupays, A. G., Jacquet, S., Audigié, F., Denoix, J. M., Laugier, P., Mitton, D., Crevier-Denoix, N., 2012a. Axial Speed of Sound for the Monitoring of Injured Equine Tendons: a Preliminary Study. Journal of Biomechanics 45, 53-58.

Vergari, C., Pourcelot, P., Ravary-Plumioën, B., Dupays, A. G., Denoix, J. M., Mitton, D., Laugier, P., Crevier-Denoix, N., 2012b. First Application of Axial Speed of Sound to Follow up Injured Equine Tendons. Ultrasound in Medicine & Biology 38, 162-167.

Viidik, A., Lewin, T., 1966. Changes in tensile strength characteristics and histology of rabbit ligaments induced by different modes of postmortal storage. Acta Orthopaedica Scandinavica 37, 141-155.

Woo, S. L., Orlando, C. A., Camp, J. F., Akeson, W. H., 1986. Effects of postmortem storage by freezing on ligament tensile behavior. Journal of Biomechanics 19, 399-404.